Available online at www.sciencedirect.com
ScienceDirect
Trans. Nonferrous Met. Soc. China 32(2022) 333−344
Transactions of Nonferrous Metals Society of China
www.tnmsc.cn

Recovery of Fe, V, and Ti in modified Ti-bearing blast furnace slag

Ji-qing HAN[1], Jing ZHANG[1], Jia-hao ZHANG[1], Xiao CHEN[2], Li ZHANG[1], Gan-feng TU[1]

1. School of Metallurgy, Northeastern University, Shenyang 110819, China;
2. School of Materials Science and Engineering, Northeastern University, Shenyang 110819, China

Received 20 December 2020; accepted 10 August 2021

Abstract: A two-stage oxidation—alkali leaching—acid leaching method was proposed to recovery Fe, V, and Ti in modified Ti-bearing blast furnace slag. The optimal experiment conditions of iron extraction were one-stage oxidation time 40 s and holding time 8 min. The recovery rate of iron was 89.93%. The optimum experiment conditions of vanadium extraction were total oxidation time of 126 s, NaOH concentration of 4.0 mol/L, leaching temperature of 95 °C, leaching time of 90 min, and the number of cycle was 4. The leaching rate of vanadium was 92.13%. The optimal experiment conditions of titanium extraction were HCl concentration of 4.5 mol/L, leaching temperature of 75 °C, and leaching time of 90 min. The TiO_2 content of synthetic rutile was 98.61%.
Key words: Ti-bearing blast furnace slag; oxidation; modification; leaching; synthetic rutile; pig iron

1 Introduction

China is rich in titanium resources, 95% of which are stored in the form of vanadium−titanium magnetite in the southwestern part of the country [1−3]. Currently, ore containing about 30% Fe, 10% TiO_2, and 0.3% V_2O_5 is smelted in blast furnaces at the Panzhihua Iron and Steel Corporation. Most Ti components in the ore are separated from iron and are enriched in the molten slag (22%−25% TiO_2). More than 3 million tons of blast furnace slag are generated yearly in China. In the last few years, several methods for treating the slag have been studied, such as flotation separation, magnetic separation, hydrometallurgy and pyrometallurgy [4]. Nevertheless, the recovery efficiency of Ti components of those methods is relatively low, and the slag has not been used efficiently [5]. Owing to the dispersive distribution of Ti constituents in various fine-grained (<10 μm) mineral phases with complex interfacial combinations, it is difficult to recover them via traditional separation methods.

Therefore, a method for the selective crystallization and separation of perovskite phase was proposed [6]. There are many studies [7−13] on enriching the titanium components in blast furnace slag into perovskite. Nevertheless, it has been proved that perovskite is different to be extracted due to its dendrite structure and the similar density with other phases. Compared to perovskite (density: 4.0 g/cm^3), rutile possesses a high added value and high density (4.2−4.3 g/cm^3). Therefore, it is appropriate to enrich Ti components to rutile phase. There is some research on the selective precipitation and separation of rutile phase. LI et al [14] investigated the crystallization behavior of rutile phase in modified titanium-bearing blast furnace slag. SUN et al [15] investigated the effect of P_2O_5 and basicity on the crystallization behaviors of rutile phase in modified titanium-bearing blast furnace slag using the single hot thermocouple technique. ZHANG et al [16] studied the crystallization and coarsening kinetics of rutile in modified titanium-bearing blast furnace slag.

Corresponding author: Li ZHANG, Tel: +86-24-83687750, E-mail: fantai320@163.com
DOI: 10.1016/S1003-6326(22)65798-4

ZHANG et al [17] proved the feasibility of alkali leaching — acid leaching of modified titanium-bearing blast furnace slag by potential−pH diagrams for extracting rutile. It is worth noting that most of the existing researches have focused on the crystallization and extraction of rutile phase in modified titanium-bearing blast furnace, but little for the extraction of metallic iron. ZHANG et al [18] studied the procedure to extract titanium components and metallic iron from modified titanium-bearing blast furnace slag. WANG et al [19] investigated the separation of iron droplets from modified titanium-bearing blast furnace slag. In the above two studies, all O_2 was blown into the molten slag at one time to oxidize high melting point substances (TiC and TiN), thereby reducing the viscosity of the molten slag and realizing the settlement of metallic iron. The TiO_2 contents of the modified titanium-bearing blast furnace slag of the above two studies are less than 30%. There are no reports about the research of extraction of metallic iron from modified titanium-bearing blast furnace slag with a high TiO_2 content (47%).

This study aimed to explore the recovery of Fe, V, and Ti in modified Ti-bearing blast furnace slag by two-stage oxidation—alkali leaching—acid leaching. The oxidation, alkali leaching, and acid leaching conditions were optimized by single-factor experiments. Moreover, the mechanisms of extraction of metallic iron and vanadium were discussed.

2 Experimental

2.1 Materials

In this study, Ti-bearing blast furnace slag was purchased from Panzhihua Iron and Steel Research Institute (Sichuan province, China). Based on previous research [20], titanium slag was prepared from titanium middling ore. The additive, SiO_2, was of analytical grade and provided by China National Medicines Corporation Ltd. The O_2 with a purity of 99% (mass fraction) was provided by Shenyang Shuntai Gas Corporation Ltd. The chemical compositions and XRD patterns of Ti-bearing blast furnace slag and titanium slag are shown in Table 1 and Fig. 1, respectively. It can be seen that Ti-bearing blast furnace slag mainly contains perovskite ($CaTiO_3$), akermanite ($Ca_2MgSi_2O_7$), diopside ($CaMgSi_2O_6$), and spinel ($MgAl_2O_4$). Anosovite and anorthite ($CaAl_2(SiO_4)_2$) are the main phases in titanium slag.

2.2 Procedures

2.2.1 Extraction of metallic iron

To study the mechanism of extraction of metallic iron, the standard Gibbs free-energy changes of relevant reactions were calculated by

Table 1 Chemical components of samples (wt.%)

Sample No.	CaO	SiO_2	TiO_2	Ti_2O_3	Al_2O_3	MgO	FeO	MFe	V_2O_5	TiC+TiN
1	26.87	25.13	17.58	3.86	14.08	7.86	1.51	2.18	0.21	0.57
2	4.32	8.85	60.72	14.65	2.64	2.02	−	0.96	3.05	0.32

1: Ti-bearing blast furnace slag; 2: Titanium slag; MFe represents metallic iron content

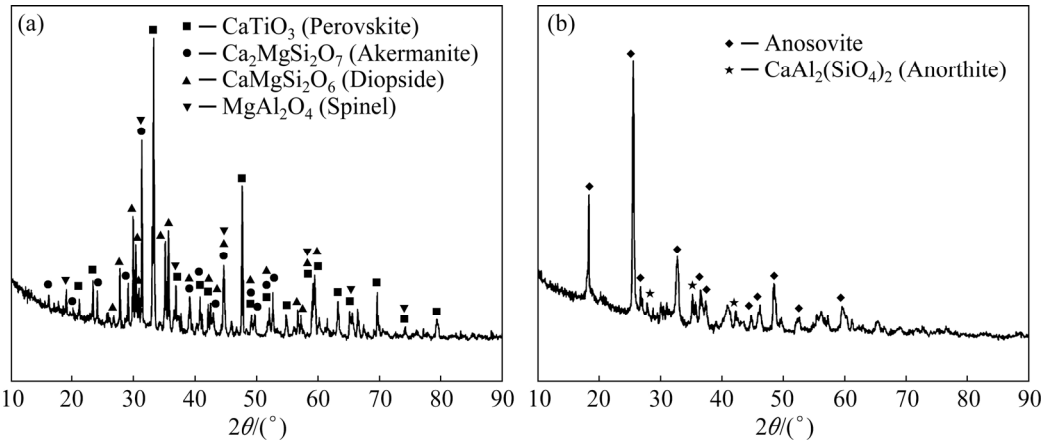

Fig. 1 XRD patterns of raw materials: (a) Ti-bearing blast furnace slag; (b) Titanium slag

FactSage. Further, the effect of oxidation time on the crystallization behavior of titanium-bearing mixed molten slag (titanium-bearing blast furnace slag and titanium slag) was simulated by FactSage. The Scheil-Gulliver cooling method in the Equilib module of FactSage was used to build the relationship between oxidation time and crystallized phases. To verify the authenticity of simulation results, the molten slags with one-stage oxidation time of 0, 42, 84, and 126 s were quenched in water.

The modification experiments were performed in a vertical $MoSi_2$ furnace with a B-type thermocouple. It was estimated that the overall temperature accuracy of the experiment was ±3 °C. The oxidation gas was O_2, and the flow rate of O_2 was 5 L/min. The O_2 was blown into molten slag twice. According to the previous research [21,22], the added mass of titanium-bearing blast furnace slag, the added mass of titanium slag, the added mass of SiO_2 and the total oxidation time were 222 g, 278 g, 40 g, and 126 s, respectively. The above raw materials were loaded into a crucible at 1450 °C for 20 min to melt fully, and then O_2 was blown into molten slag with a certain time (10, 20, 30, 40, 50, 60, 70, 80, 90, and 100 s). The oxidized molten slag was kept at 1450 °C for a specified time (2, 4, 6, 8, 10 and 12 min), and then the remaining O_2 was blown into molten slag. Subsequently, molten slag was slowly cooled to room temperature at a cooling rate of 5 °C/min. The cooled slag was called modified titanium-bearing blast furnace slag (MTBBFS). The mass of pig iron was weighed, and the content of metallic iron in the MTBBFS was analyzed. The purpose of modification experiments was to transform the titanium-bearing phases (perovskite and anosovite) in the raw materials (titanium-bearing blast furnace slag and titanium slag) into rutile phase. The rutile was the raw material of titanium white with the chloride process. The schematic diagram of the experimental process is shown in Fig. 2.

2.2.2 Extraction of vanadium

The modified experiments were carried out under the optimum conditions of iron extraction experiments, i.e., the O_2 was blown into molten slag with an oxidation time of 40 s, and then the oxidized molten slag was held at 1450 °C for 8 min. Subsequently, the remaining O_2 (44, 65, 86, 107, 128, and 149 s) was blown into molten slag and the slag was slowly cooled to room temperature at a cooling rate of 5 °C/min. Before alkali leaching, the modified slag was first ground to a particle size of less than 150 μm.

The experiments of alkali leaching were performed at atmospheric pressure in a 500 mL three-necked flask equipped with a reflux condenser. The reaction mixture was heated by a thermostatic water bath and agitated by a magnetic stirrer at a

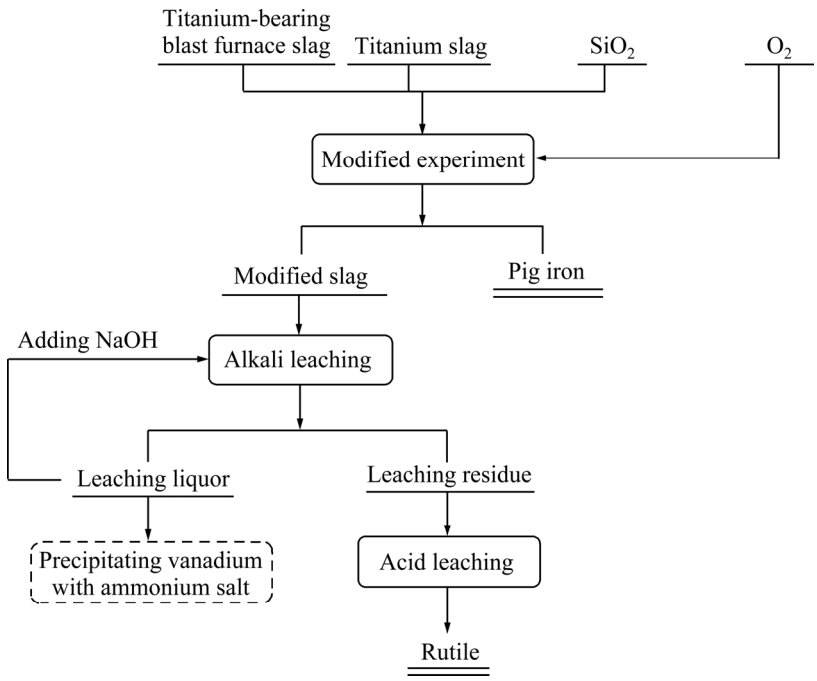

Fig. 2 Schematic diagram of experimental process

stirring rate of 500 r/min. For each experiment, the added mass of the MTBBFS was 100 g, and the liquid−solid ratio was fixed at 3 (mL/g).

According to a L/S of 3 (mL/g), the volume of alkali-leaching solution was 300 mL. Then, a concentration of NaOH solution (1.0−4.0 mol/L) was taken and poured into a three-necked flask. Once the specified temperature (25−95 °C) was reached, the MTBBFS was added to the reactor and leached for a certain time (30−180 min). Afterwards, the slurry was filtered to separate leaching residue from leaching liquor. The leaching residue was washed repeatedly with the distilled water until the washing fluid was neutral. The leaching liquor was first submitted for chemical analysis, and then was recycled by adding 30 g NaOH for the next alkali leaching. The leaching rate (η) of V was calculated with Eq. (1):

$$\eta=\frac{m_{\mathrm{L}}}{m_0}\times 100\% \quad (1)$$

where m_{L} is the mass of element in leaching liquor, and m_0 is the mass of element in the MTBBFS.

2.2.3 Extraction of titanium

Before acid (HCl) leaching, the MTBBFS was first leached under the above optimal alkali (NaOH) leaching conditions. Then, the product of alkali leaching was leached by hydrochloric acid. The leaching residue was washed with distilled water, dried in an oven at 110 °C for 24 h, and submitted for chemical analysis. The experimental conditions of acid leaching: HCl concentration 2.0−5.0 mol/L, leaching temperature 25−85 °C, leaching time 30−180 min, a liquid−solid ratio of 3 (mL/g), and 100 g of alkali-leaching product.

2.3 Characterization

The chemical compositions of relevant samples were analyzed by Inductively Coupled Plasma-Atomic Emission Spectroscopy (ICP-AES, PerkinElmer Optima 4300DV). The ammonium ferric sulfate titration method [23] was used to determine the content of TiO_2. The potassium dichromate titration method [24] was used to determine the content of Ti_2O_3. According to the relevant references [25,26], the total content of TiC and TiN in the raw materials was determined. The phase compositions of relevant samples were identified by XRD analysis (X'PERT PROMPD/PW3040, PANalytical B.V. Corp., The Netherlands) using Cu K_α radiation for 7 min from 10° to 90°. The microscopic observation and element distribution of relevant samples were conducted by using a scanning electron microscopy (TESCAN VEGA III) equipped with an EDS spectrometer (INCA Energy 350). The viscosity of molten slag was measured through the rotating spindle method by the ZCN−1600 melt physical property comprehensive testing instrument with a digital viscometer. Quenched samples were observed by a metallographic microscope (201A-D). The standard Gibbs free energy changes of relevant reactions were calculated by the reaction module of FactSage software (version 7.1). The Equilib module of FactSage was used to build the relationship between oxidation time and the mass of crystallized phases. The Pourbaix diagrams of V−Ti−H_2O systems at 25 and 100 °C were drawn by the E−pH module of FactSage. The databases of FactSage used in the above thermodynamic calculation were FToxid and FactPS.

3 Results and discussion

3.1 Extraction of metallic iron

3.1.1 Extraction mechanism of metallic iron

To study the mechanism of extraction of metallic iron, the standard Gibbs free-energy changes of relevant reactions were calculated, and the results are shown in Fig. 3. It is well known that the reason for the high melting points of titanium-bearing blast furnace slag and titanium slag is that they contain high melting point substances, such as TiC and TiN. As shown in Fig. 3, the standard

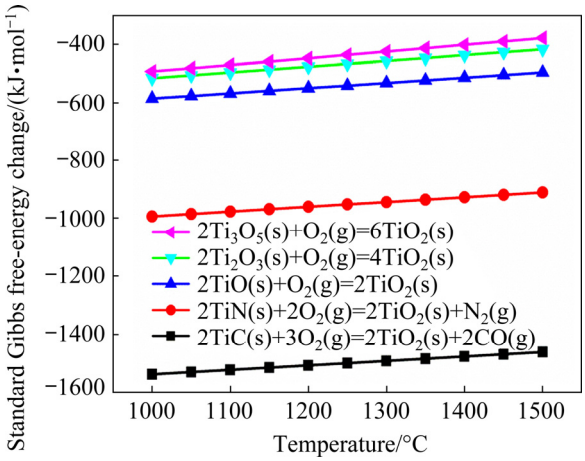

Fig. 3 Standard Gibbs free-energy changes of relevant reactions

Gibbs free-energy changes of the oxidation reactions of TiC and TiN are less than those of TiO, Ti_2O_3, and Ti_3O_5, implying that TiC and TiN are preferentially oxidized to TiO_2 when O_2 is blown into molten slag. The disappearance of TiC and TiN will result in a decrease in the viscosity of molten slag. While a decrease in the viscosity of molten slag is beneficial to the settling of metallic iron particles.

When all O_2 (total oxidation time 126 s) was blown into molten slag for one time, the SEM image and XRD pattern of the MTBBFS are shown in Fig. 4. It can be seen that the metallic iron was not settled. According to the previous research [21], when the content of TiO_2 in the raw materials was 29.17 wt.% and all O_2 was passed into molten slag for one time, metallic iron particles were settled to the bottom of the slag. We guessed that the TiO_2 content of the raw materials in this study increasing to 47 wt.% causes a large amount of rutile crystals to crystallize at 1450 °C, which increases the viscosity of molten slag and metallic iron particles could not be settled. Therefore, we would verify this conjecture through both theory and experiments.

The Scheil−Gulliver cooling method in the Equilib module of FactSage was used to build the relationship between oxidation time and the mass of crystallized phases, and the results are shown in Figs. 5 and 6. The relationship between the

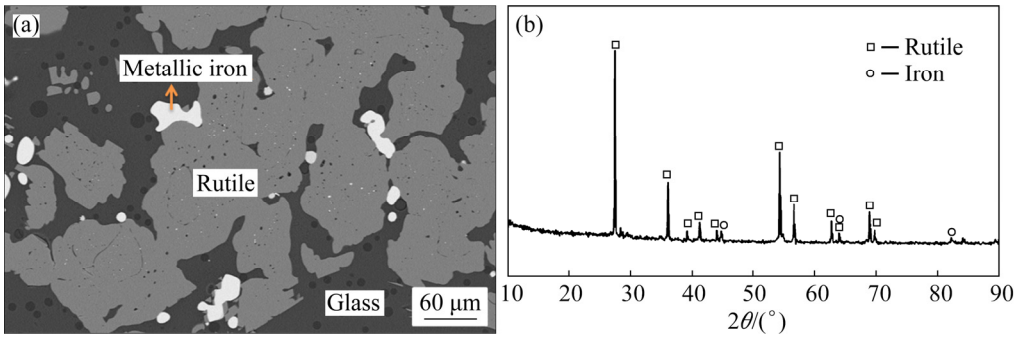

Fig. 4 SEM image (a) and XRD pattern (b) of MTBBFS

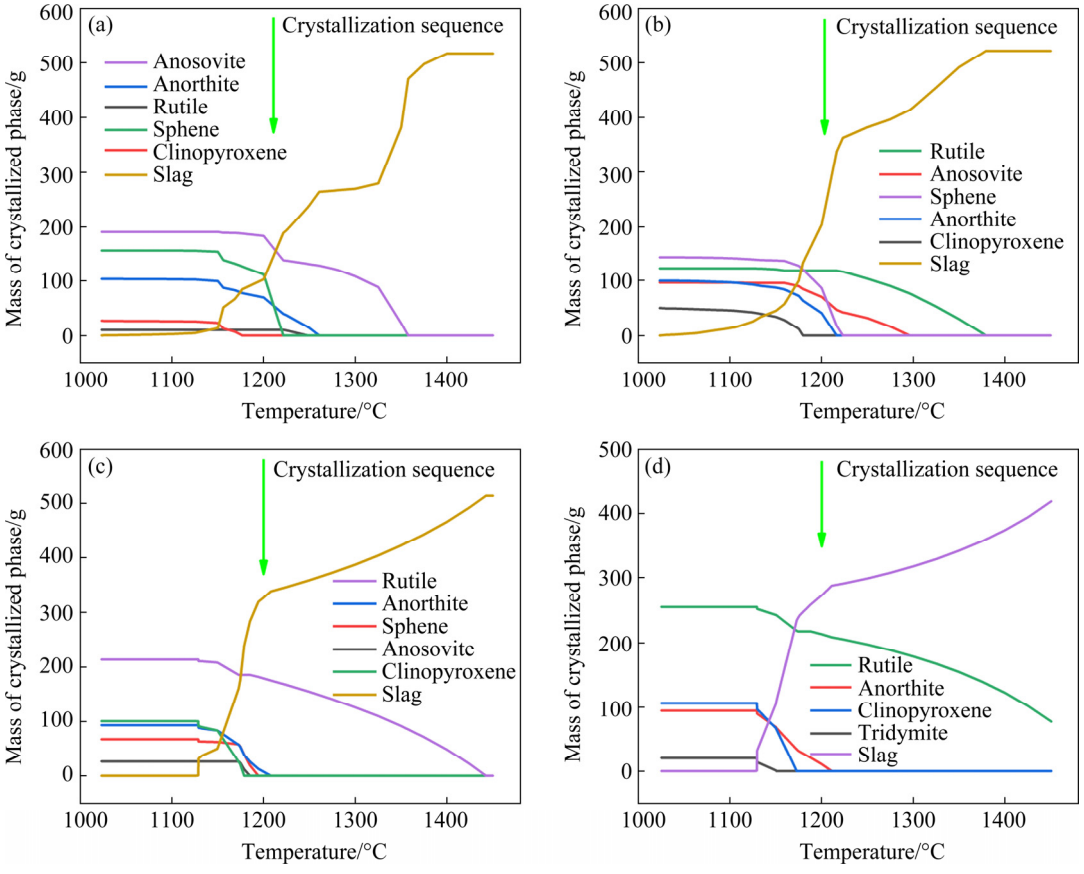

Fig. 5 Relationship between oxidation time and mass of crystallized phases: (a) 0 s; (b) 42 s; (c) 84 s; (d) 126 s

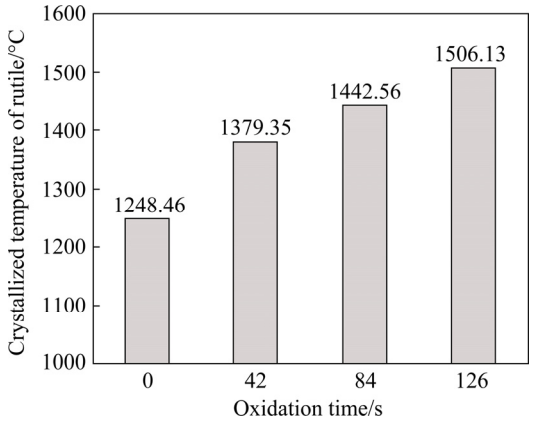

Fig. 6 Relationship between crystallized temperature of rutile and oxidation time

crystallized temperature of rutile and oxidation time is illustrated in Fig. 6, and the relationship between the mass of crystallized rutile at 1450 °C and oxidation time is shown in Fig. 7. As shown in Figs. 5 and 6, when oxidation time was 0 s, the crystallized order of mineral phases in the MTBBFS was anosovite → anorthite → rutile → sphene → clinopyroxene. The first crystallized phase was anosovite and the crystallized temperature was 1357.62 °C. When oxidation time was 42 s, the crystallized order of phases in the MTBBFS was rutile → anosovite → sphene → anorthite → clinopyroxene. The first crystallized phase was rutile and the crystallized temperature was 1379.35 °C. When oxidation time was 84 s, the crystallized order of phases in the MTBBFS was rutile → anorthite → sphene → anosovite → clinopyroxene. The first crystallized phase was rutile and the crystallized temperature was 1442.56 °C. When oxidation time was 126 s, the crystallized order of phases in the MTBBFS was rutile → anorthite → clinopyroxene → tridymite. The first crystallized phase was rutile and the crystallized temperature was 1506.13 °C. As shown in Figs. 6 and 7, rutile crystals precipitated at 1450 °C when the oxidation time was 126 s. In summary, the crystallized temperature of rutile was greater than 1450 °C when the oxidation time was 126 s, implying that rutile crystallized at 1450 °C.

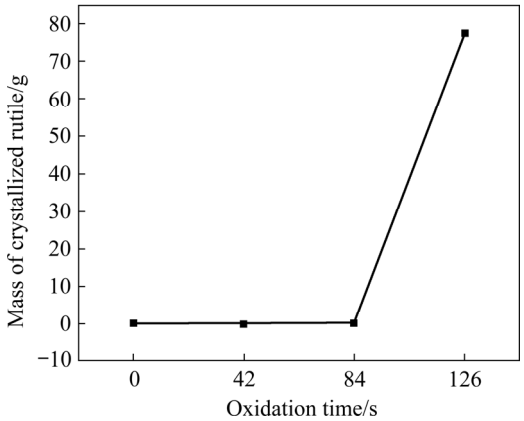

Fig. 7 Relationship between mass of crystallized rutile at 1450 °C and oxidation time

As shown in Fig. 8, when oxidation time was 0, 42, and 84 s, no rutile crystals were found in the quenched samples. When oxidation time increased to 126 s, rutile crystals were observed in the quenched sample. The above results indicate that rutile crystals crystallized when oxidation time was 126 s. The crystallization of rutile crystals led to an increase in the viscosity of molten slag, which inhibited the settling of metallic iron particles.

3.1.2 Extraction experiments of metallic iron

The effect of one-stage oxidation time on the content of metallic iron in the MTBBFS and the recovery rate of metallic iron is shown in Fig. 9(a). With one-stage oxidation time increasing from 10 to 40 s, the content of metallic irons decreased and the recovery rate of metallic iron increased. As one-stage oxidation time increased from 40 to 90 s, the content of metallic iron and the recovery rate of metallic iron remained unchanged. When one-stage oxidation time increased from 90 to 100 s, the content of metallic iron increased, while the recovery rate of metallic iron decreased. Thus, the optimal one-stage oxidation time was 40 s.

Figure 9(b) shows the effect of holding time on the content of metallic iron and the recovery rate of metallic iron. As holding time increased from 2 to 8 min, the content of metallic iron decreased and the recovery rate of metallic iron increased. With holding time increasing from 8 to 12 min, the content of metallic iron and the recovery rate of metallic iron remained unchanged. Therefore, the optimum holding time was 8 min.

The relationship between total oxidation time and viscosity is illustrated in Fig. 10. With oxidation time increasing from 0 to 42 s, the viscosity of molten slag decreased. This is because TiC and TiN in the raw materials were oxidized, leading to a decrease in the viscosity of molten slag. Thus, the recovery rate of metallic iron increased and the content of metallic iron decreased when oxidation time increased from 0 to 40 s. As oxidation time increased from 42 to 126 s, the

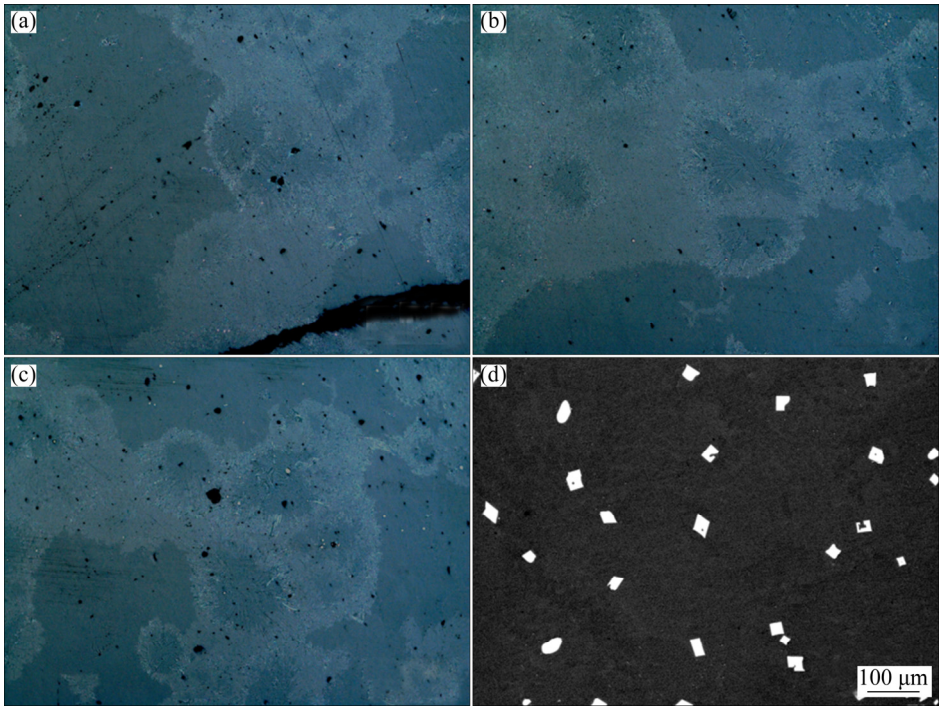

Fig. 8 Metallographic microscope images of quenched samples with different oxidation time: (a) 0 s; (b) 42 s; (c) 84 s; (d) 126 s

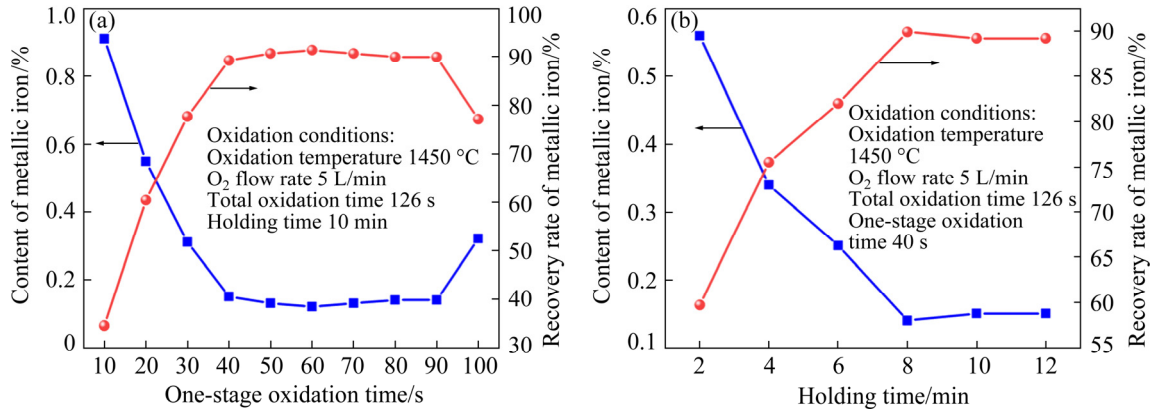

Fig. 9 Effects of one-stage oxidation time (a) and holding time (b) on content of metallic iron in MTBBFS and recovery rate of metallic iron

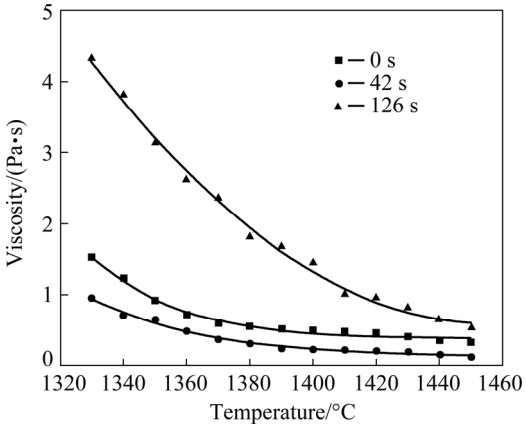

Fig. 10 Relationship between total oxidation time and viscosity

viscosity of molten slag increased. This is because a large amount of rutile crystals precipitated when oxidation time was 126 s. Therefore, the recovery rate of metallic iron decreased and the content of metallic iron increased when oxidation time increased from 90 to 100 s.

In summary, the optimal experiment conditions of iron extraction were one-stage oxidation time of 40 s and holding time of 8 min. The recovery rate of iron was 89.93% and the metallic iron content of the MTBBFS was 0.14%. The chemical compositions of vanadium-containing pig iron are listed in Table 2. Table 2 reveals that the contents of Fe and V in the vanadium-containing pig iron

were 94.46 wt.% and 0.33 wt.%, respectively. The product can be used as a raw material for converter to obtain vanadium slag and semi-steel.

Table 2 Chemical compositions of vanadium-containing pig iron (wt.%)

Fe	C	Si	V	Mn	Ti	S	P
94.46	4.31	0.35	0.33	0.28	0.14	0.072	0.058

3.2 Extraction of vanadium

3.2.1 Extraction mechanism of vanadium

To investigate the extraction mechanism of vanadium element, the standard Gibbs free-energy changes of oxidation reactions at 1000−1500 °C were calculated, and the Pourbaix diagrams of V−Ti−H_2O systems at 25 and 100 °C were drawn. The results are presented in Figs. 11 and 12. When O_2 is blown into molten slag, the oxidation sequence of titanium, iron, and vanadium oxides is presented in Fig. 11. At 1450 °C, it can be observed that Ti, TiO, Ti_2O_3, and Ti_3O_5 are first oxidized to TiO_2. In the meantime, V and VO are oxidized into V_2O_3. And then Fe and FeO are oxidized to Fe_3O_4. Finally, V_2O_3 and VO_2 are oxidized to V_2O_5. Since titanium slag and Ti-bearing blast furnace slag mainly contain trivalent titanium, metallic iron, and trivalent vanadium, the oxidation order is $Ti_2O_3 \rightarrow Fe \rightarrow V_2O_3$.

As shown in Fig. 12, VO_2 is leached by acid in form of VO^{2+}. The V_2O_5 is removed by alkali in form of HVO_4^{2-}, while VO and V_2O_3 are not leached by acid or alkali. With temperature increasing from 25 to 100 °C, the stable area of VO^{2+} decreases, while that of HVO_4^{2-} increases, implying that an increase in temperature can decrease the required pH of the alkali leaching of V_2O_5. It is worth noting that titanium element always exists as TiO_2 in the pH range of 0−14. In this work, vanadium and titanium elements in the MTBBFS are in the form of V_2O_5 and TiO_2, respectively. Therefore, V_2O_5 can be leached by alkali, while TiO_2 is enriched in the leaching residue.

3.2.2 Extraction experiments of vanadium

The effects of total oxidation time on the leaching rate of vanadium are shown in Fig. 13(a). When total oxidation time increased from 84 to

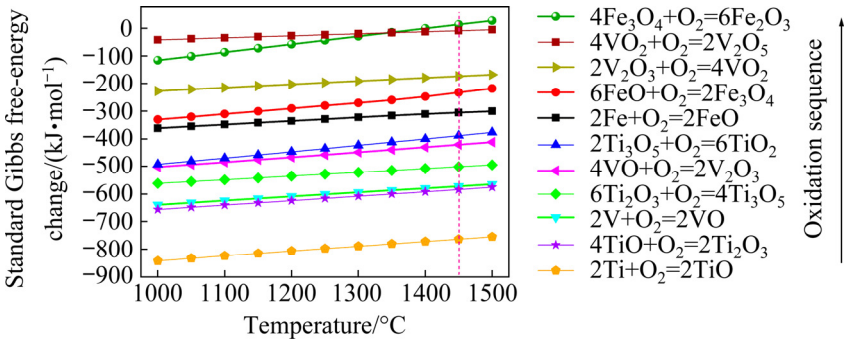

Fig. 11 Standard Gibbs free-energy changes of oxidation reactions at 1000−1500 °C

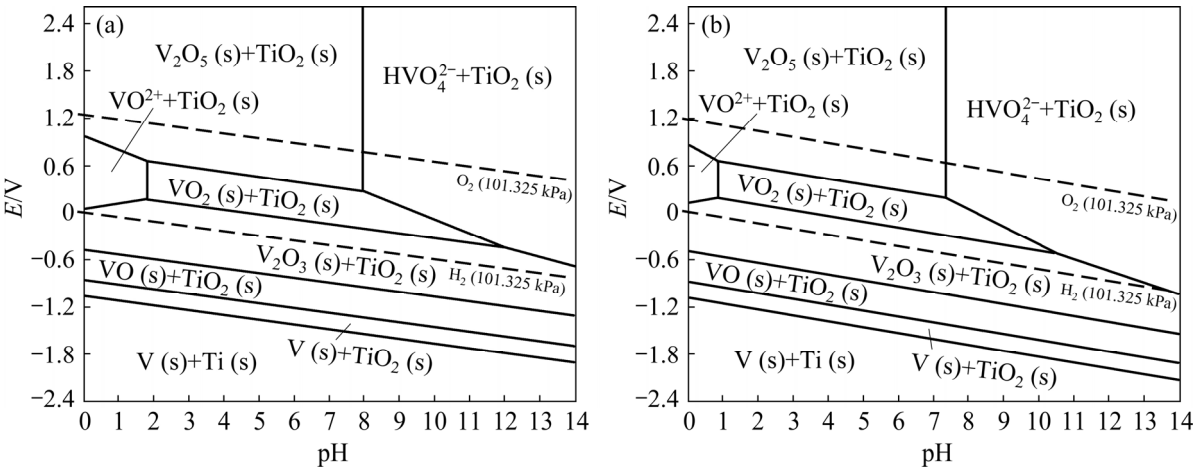

Fig. 12 Pourbaix diagrams of V−Ti−H_2O systems at 25 °C (a) and 100 °C (b)

105 s, the leaching rate of vanadium slightly increased. With total oxidation time increasing from 105 to 126 s, the leaching rate of vanadium rapidly increased. It can be seen from Fig. 11 that the reason for a rapid increase is that low-valence titanium elements were first oxidized, and then low-valence vanadium elements were oxidized. As total oxidation time increased from 126 to 189 s, the leaching rate of vanadium remained unchanged. Therefore, the optimal total oxidation time was 126 s. The effects of NaOH concentration on the leaching rate of vanadium are shown in Fig. 13(b). As NaOH concentration increased from 2.5 to 4.0 mol/L, the leaching rate of vanadium significantly increased. With NaOH concentration increasing from 4.0 to 5.5 mol/L, the leaching rate of vanadium was almost constant. Thus, the optimum NaOH concentration was 4.0 mol/L. Figure 13(c) shows the effects of leaching temperature on the leaching rate of vanadium. The leaching rate of vanadium increased with leaching temperature increasing. Thus, the optimal leaching temperature was 95 °C. The effects of leaching time on the leaching rate of vanadium are shown in Fig. 13(d). As leaching time increased from 30 to 180 min, the leaching rate of vanadium first increased and then remained unchanged. Therefore, the optimum leaching time was 90 min.

The relationship between the number of cycle and the leaching rate of vanadium is illustrated in Fig. 14. When the number of cycle increased from 1 to 4, the leaching rate of vanadium was almost constant (about 92%) and the concentration of vanadium in leaching liquor increased. With the number of cycle increasing from 4 to 5, the concentration of vanadium continued to increase, but the leaching rate of vanadium markedly decreased. Thus, the optimal number of cycle was 4.

In summary, the optimal alkali leaching conditions were total oxidation time 126 s, NaOH

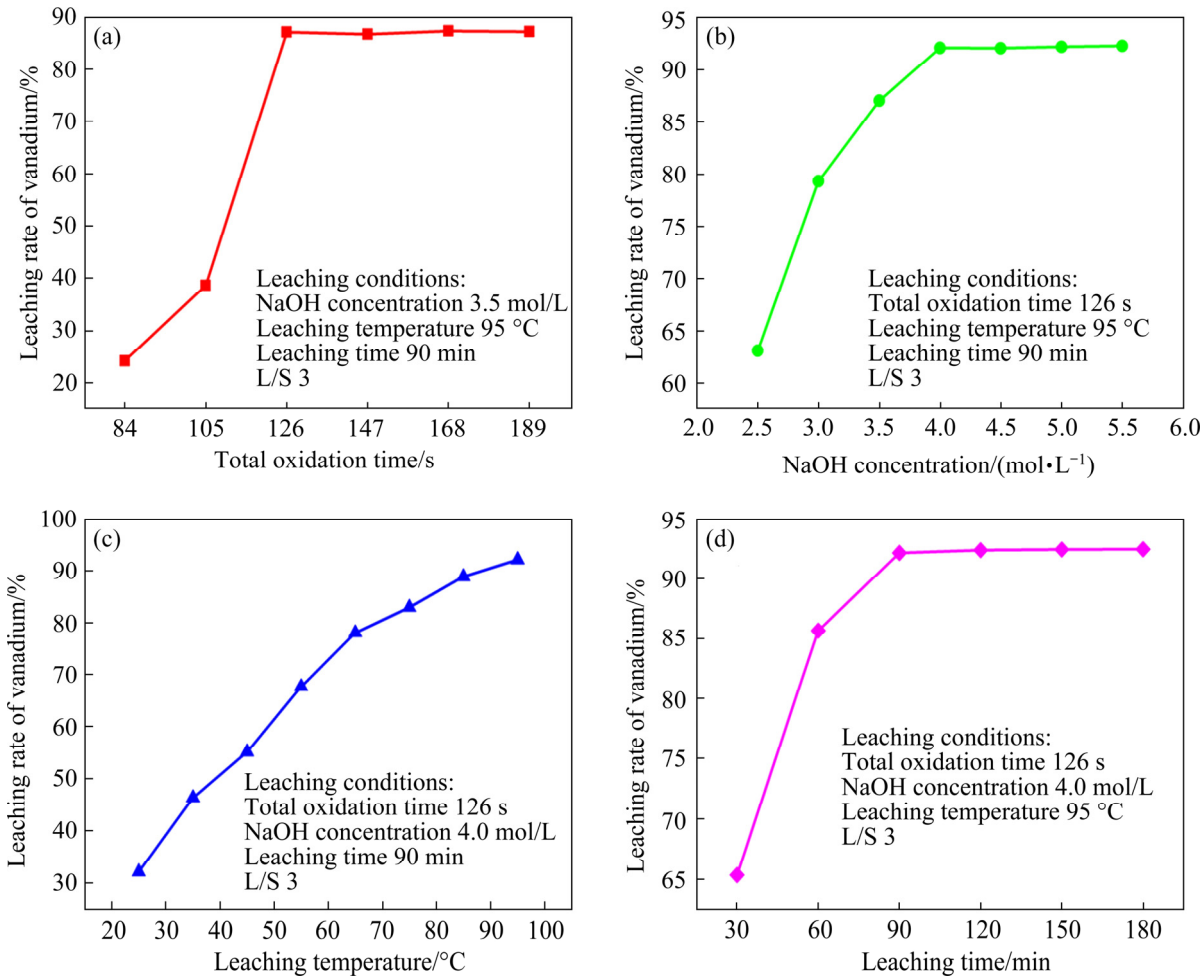

Fig. 13 Effects of total oxidation time (a), NaOH concentration (b), leaching temperature (c), and leaching time (d) on leaching rate of vanadium

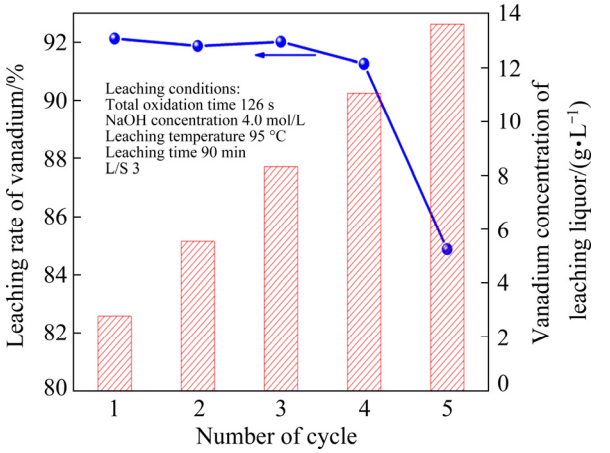

Fig. 14 Relationship among number of cycle, leaching rate of vanadium, and vanadium concentration of leaching liquor

concentration 4.0 mol/L, leaching temperature 95 °C, leaching time 90 min, and the number of cycle 4. The circulating leaching solution could be used to recover vanadium by the precipitation of ammonium salt. The chemical components of the residue after alkali leaching are listed in Table 3. Table 3 reveals that the contents of SiO_2, Al_2O_3 and V_2O_5 are 0.29%, 0.12%, and 0.15%, respectively, implying that most SiO_2, Al_2O_3 and V_2O_5 were leached by alkali. Therefore, the TiO_2 content of leaching residue increased to 72.84%.

Table 3 Chemical compositions of residue after alkali leaching (wt.%)

TiO_2	SiO_2	CaO	Al_2O_3	MgO	Fe_2O_3	V_2O_5
72.84	0.29	19.13	0.12	6.51	0.22	0.15

3.3 Extraction of titanium

The effect of HCl concentration on TiO_2 content is shown in Fig. 15(a). As HCl concentration increased from 2.0 to 4.5 mol/L, TiO_2 content significantly increased. When HCl concentration increased from 4.5 to 5.0 mol/L, TiO_2 content slightly increased. Thus, the optimal HCl concentration was 4.5 mol/L. Figure 15(b) illustrates the effect of leaching temperature on TiO_2 content. With leaching temperature increasing from 25 to 75 °C, TiO_2 content rapidly increased. As leaching temperature increased from 75 to 85 °C, TiO_2 content was almost constant. Thus, the optimum leaching temperature was 75 °C. Figure 15(c) shows the effect of leaching time on TiO_2 content. As leaching time increased from 30 to

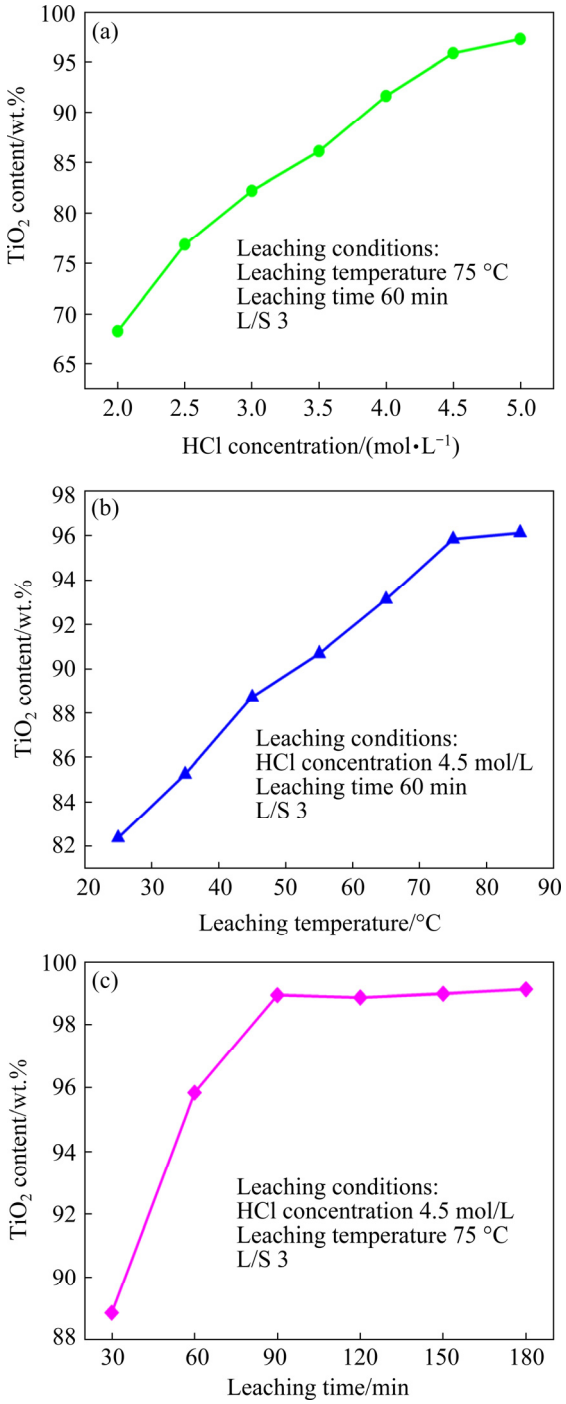

Fig. 15 Effects of HCl concentration (a), leaching temperature (b), and leaching time (c) on TiO_2 content

90 min, TiO_2 content markedly increased. When leaching time increased from 90 to 180 min, TiO_2 content remained unchanged. Therefore, the optimal leaching time was 90 min.

In a word, the optimum acid leaching conditions were HCl concentration 4.5 mol/L, leaching temperature 75 °C, and leaching time 90 min. The TiO_2 content of synthetic rutile was 98.61%, and its total content of CaO and MgO was

0.41%. The phase and micromorphology of synthetic rutile are presented in Fig. 16. The chemical compositions of synthetic rutile are listed in Table 4. Due to the TiO_2 content more than 98% and the total content of CaO and MgO less than 0.5%, the synthetic rutile was a high-quality feedstock for titanium white with the chloride process.

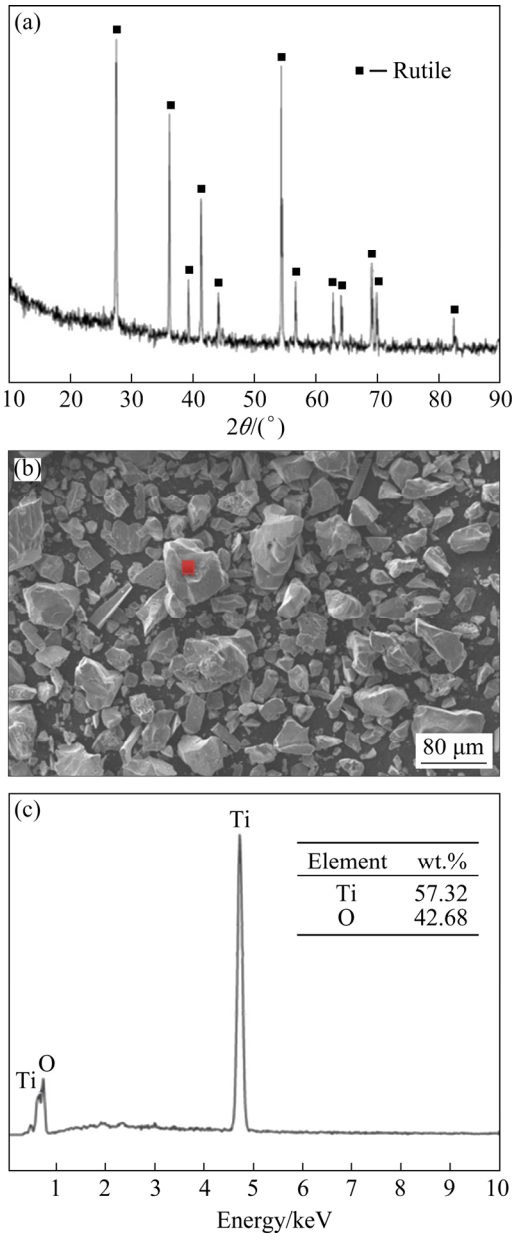

Fig. 16 Characterization of synthetic rutile: (a) XRD pattern; (b) SEM image; (c) EDS analysis

Table 4 Chemical compositions of synthetic rutile (wt.%)

TiO_2	SiO_2	CaO	Al_2O_3	MgO	Fe_2O_3	V_2O_5
98.61	0.32	0.24	0.07	0.17	0.15	0.19

4 Conclusions

(1) The optimal experiment conditions of iron extraction are one-stage oxidation time of 40 s and holding time of 8 min. The recovery rate of iron is 89.93% and the metallic iron content of the MTBBFS is 0.14 wt.%.

(2) The optimum experiment conditions of vanadium extraction are total oxidation time of 126 s, NaOH concentration of 4.0 mol/L, leaching temperature of 95 °C, leaching time of 90 min, and the number of cycle 4. The leaching rate of vanadium is 92.13%.

(3) The optimal experiment conditions of titanium extraction are HCl concentration of 4.5 mol/L, leaching temperature of 75 °C, and leaching time of 90 min. The TiO_2 content of synthetic rutile is 98.61 wt.%, and the total content of CaO and MgO is 0.41 wt.%.

(4) Due to the TiO_2 content more than 98 wt.% and the total content of CaO and MgO less than 0.5 wt.%, the product is a high-quality rutile for titanium white with the chloride process.

Acknowledgments

The authors are grateful for the financial support from the National Science and Technology Support Program of China (No. 2015BAB18B00).

References

[1] DU He-gui. Theory of smelting V and Ti-magnetite by blast furnace [M]. Beijing: Science Press, 1996. (in Chinese)

[2] FENG Cong, GAO Li-hua, TANG Jue, LIU Zheng-gen, CHU Man-sheng. Effects of MgO/Al_2O_3 ratio on viscous behaviors and structures of $MgO−Al_2O_3−TiO_2−CaO−SiO_2$ slag systems with high TiO_2 content and low CaO/SiO_2 ratio [J]. Transactions of Nonferrous Metals Society of China, 2020, 30(3): 800−811.

[3] WANG Shuai, GUO Yu-feng, ZHENG Fu-qiang, CHEN Feng, YANG Ling-zhi, JIANG Tao, QIU Guan-zhou. Behavior of vanadium during reduction and smelting of vanadium titanomagnetite metallized pellets [J]. Transactions of Nonferrous Metals Society of China, 2020, 30(6): 1687−1696.

[4] LI Liao-sha, SUI Zhi-tong. Physical chemistry behavior of enrichment selectivity of TiO_2 in perovskite [J]. Acta Physico-Chimica Sinica, 2001, 17(9): 845−849. (in Chinese)

[5] LI Liao-sha, LOU Tai-ping, CHE Chang-yin, SUI Zhi-tong. Kinetics on the oxidation of $CaO−SiO_2−Al_2O_3−MgO−TiO_x−FeO_y$ system [J]. Acta Physico-Chimica Sinica, 2000, 16(8): 708−712. (in Chinese)

[6] WANG Xi-dong, MAO Yu-wen, LIU Xiang-ying, ZHU

Yuan-kai. Study on crystallization behavior of blast furnace slag containing TiO_2 [J]. Journal of Iron and Steel Research, 1990, 2(3): 1−6. (in Chinese)
[7] ZHANG Li, ZHANG Lin-nan, WANG Ming-yu, LOU Tai-ping, SUI Zhi-tong, JANG Jing-shi. Effect of perovskite phase precipitation on viscosity of Ti-bearing blast furnace slag under the dynamic oxidation condition [J]. Journal of Non-Crystalline Solids, 2006, 352(2): 123−129.
[8] ZHANG Li, ZHANG Lin-nan, WANG Ming-yu, LI Guang-qiang, SUI Zhi-tong. Precipitation selectivity of perovskite phase from Ti-bearing blast furnace slag under dynamic oxidation conditions [J]. Journal of Non-Crystalline Solids, 2007, 353(22/23): 2214−2220.
[9] ZHANG Li, ZHANG Lin-nan, WANG Ming-yu, LI Guang-qiang, SUI Zhi-tong. Recovery of titanium compounds from molten Ti-bearing blast furnace slag under the dynamic oxidation condition [J]. Minerals Engineering, 2007, 20(7): 684−693.
[10] SUI Zhi-tong, ZHANG Peng-xing, YAMAUCHI C. Precipitation selectivity of boron compounds from slags [J]. Acta Materialia, 1999, 47(4): 1337−1344.
[11] WANG Ming-yu, LI Liao-sha, ZHANG Li, ZHANG Lin-nan, TU Gan-feng, SUI Zhi-tong. Effect of oxidization on enrichment behavior of TiO_2 in titanium-bearing slag [J]. Rare Metals, 2006, 25(2): 106−110.
[12] WANG Ming-yu, ZHANG Lin-nan, ZHANG Li, SUI Zhi-tong, TU Gan-feng. Selective enrichment of TiO_2 and precipitation behavior of perovskite phase in titania bearing slag [J]. Transactions of Nonferrous Metals Society of China, 2006, 16(2): 421−425.
[13] ZHANG Li, ZHANG Wu, ZHANG Ju-hua, LI Guang-qiang. Effects of additives on the phase transformation, occurrence state, and the interface of the Ti component in Ti-bearing blast furnace slag [J]. International Journal of Minerals Metallurgy and Materials, 2016, 23(9): 1029−1040.
[14] LI Jing, WANG Xi-dong, ZHANG Zuo-tai. Crystallization behavior of rutile in the synthesized Ti-bearing blast furnace slag using single hot thermocouple technique [J]. ISIJ International, 2011, 51(9): 1396−1402.
[15] SUN Yong-qi, LI Jing, WANG Xi-dong, ZHANG Zuo-tai. The effect of P_2O_5 on the crystallization behaviors of Ti-bearing blast furnace slags using single hot thermocouple technique [J]. Metallurgical and Materials Transactions B, 2014, 45(4): 1446−1455.
[16] ZHANG Wu, ZHANG Li, ZHANG Ju-hua, FENG Nai-xiang. Crystallization and coarsening kinetics of rutile phase in modified Ti-bearing blast furnace slag [J]. Industrial & Engineering Chemistry Research, 2012, 51(38): 12294−12298.
[17] ZHANG Li, ZHANG Ju-hua, ZHANG Wu, LI Guang-qiang. Thermodynamic analysis of extraction of synthetic rutile from modified slag [J]. Industrial & Engineering Chemistry Research, 2013, 52(13): 4924−4931.
[18] ZHANG Wu, ZHANG Li, LI Yu-hai, LI Xin. An environmental procedure to extract titanium components and metallic iron from Ti-bearing blast furnace slag [J]. Green Processing & Synthesis, 2015, 4(4): 307−316.
[19] WANG Ming-yu, LOU Tai-ping, ZHANG Li, SUI Zhi-tong. Separation of iron droplets from titania bearing slag [J]. Journal of Iron and Steel Research, 2008, 15(1): 45−48.
[20] HAN Ji-qing, ZHANG Jing, FENG Wei, CHEN Xiao, ZHANG Li, TU Gan-feng. A clean process to prepare high-quality acid-soluble titanium slag from titanium middling ore [J]. Minerals, 2019, 9(8): 460.
[21] HAN Ji-qing, ZHANG Jia-hao, CHEN Xiao, ZHANG Jing, ZHANG Li, TU Gan-feng. Effect of rutile crystal shapes on rutile settlement [J]. Transactions of Nonferrous Metals Society of China, 2020, 30(10): 2848−2860.
[22] HAN Ji-qing, ZHANG Jia-hao, ZHANG Jing, CHEN Xiao, ZHANG Li, TU Gan-feng. Combined effect of SiO_2 and O_2 on crystallization behavior of modified Ti-bearing blast furnace slag [J]. ACS Omega, 2020, 5(15): 8619−8628.
[23] LI Jing-ling, ZHANG Nian-ci, ZUO Ping. Measurement of titanium dioxide in titanium concentrate by ammonium ferric sulfate volumetric analysis [J]. Express Information of Mining Industry, 2003, 19(8): 9−11. (in Chinese)
[24] XU Ben-ping, YUAN Guang-zhi, LI Ming, LEI Qing-ru, YOU Bo. Determination of low valence titanium (Ti^{2+}, Ti^{3+}) in vanadium titanium blast furnace slag [J]. Iron Steel Vanadium Titanium, 1989, 10(4): 61−66. (in Chinese)
[25] DU Shi-kui, HAN Kai, WANG Shu-zhen, YU Dao-cheng. Study on the phases analysis of titanium nitride, titanium carbide, total low-valent titanium, titanium dioxide [J]. Chemical Bulletin, 1978, 4: 5−7. (in Chinese)
[26] XU Ben-ping, YAN Guang-zhi, LI Ming, LEI Qing-ru, YOU Bo. Study on the determination method of titanium carbide in vanadium titanium blast furnace slag [J]. Metallurgical Analysis, 1990, 1: 35−37. (in Chinese)

改性含钛高炉渣中铁、钒和钛的回收

韩吉庆[1]，张 晶[1]，张加豪[1]，陈 晓[2]，张 力[1]，涂赣峰[1]

1. 东北大学 冶金学院，沈阳 110819；2. 东北大学 材料科学与工程学院，沈阳 110819

摘 要：提出两段氧化—碱浸—酸浸工艺来回收改性含钛高炉渣中的铁、钒和钛。较佳的提铁实验条件为一段氧化时间 40 s 和保温时间 8 min，铁的回收率为 89.93%。较佳的提钒实验条件为总氧化时间 126 s、NaOH 浓度 4.0 mol/L、浸出温度 95 °C、浸出时间 90 min 和碱浸循环次数 4，钒的浸出率为 92.13%。较佳的提钛实验条件为 HCl 浓度 4.5 mol/L、浸出温度 75 °C 和浸出时间 90 min，人造金红石的 TiO_2 含量为 98.61%。

关键词：含钛高炉渣；氧化；改性；浸出；人造金红石；生铁

(Edited by Xiang-qun LI)